Electrical Engineering (2022) 104:67–81
https://doi.org/10.1007/s00202-021-01371-w

ORIGINAL PAPER

Lifetime estimation of grid connected $LiFePO_4$ battery energy storage systems

M. Mahesh[1] · D. Vijaya Bhaskar[1] · R. K. Jisha[2] · Ram Krishan[3] · R. Gnanadass[4]

Received: 3 November 2020 / Accepted: 31 July 2021 / Published online: 24 August 2021

Abstract
Battery Energy Storage Systems (BESS) are becoming strong alternatives to improve the flexibility, reliability and security of the electric grid, especially in the presence of Variable Renewable Energy Sources. Hence, it is essential to investigate the performance and life cycle estimation of batteries which are used in the stationary BESS for primary grid applications. In this paper, a new approach is proposed to investigate life cycle and performance of Lithium iron Phosphate ($LiFePO_4$) batteries for real-time grid applications. The proposed accelerated lifetime model is based on real-time operational parameters of the battery such as temperature, State of Charge, Depth of Discharge and Open Circuit Voltage. Also, performance analysis of $LiFePO_4$ battery system has been carried out for different grid-scale applications. Proposed methodology helps to design the size of the battery system for particular grid applications. Applicability and reliability of the developed life cycle estimation model are demonstrated on the practical 500 kW/250kWh $LiFePO_4$ battery system installed at 230/110/22 kV grid connected substation at Puducherry, India. The real-time operational challenges are addressed and recommendations made based on the field data.

Keywords Battery energy storage system · Capacity degradation · Lithium-ion battery · Ancillary services · Frequency regulation · Energy time shift

1 Introduction

Distributed Energy Storage Systems are being promoted to become an integral part of the utility grid due to increased intermittent renewable energy penetrations into the grid. It acts as an energy buffer between generation and load by addressing imbalances due to the variable power generation and nonlinear loads. Recently, BESS attracted attention due to its faster response, higher ramp rate and modularity in size [1]. BESS became economically viable option compared to other energy storage systems, especially when it is integrated with Renewable Energy (RE) resources [2]. At present, various battery technologies are under research for the stacked applications of the grid including frequency regulation, RE energy time shift/peak shaving, RE capacity firming, voltage support/reactive power compensation, Power Quality and Reliability test, etc. Li-ion group attracted more attention due to its faster response, higher power and energy density, intrinsic safety and longer life [3]. Due to its faster response and higher power density, Li-ion batteries are suitable for Primary Frequency Regulation (PFR) and other ancillary services

✉ M. Mahesh
mahesh.m9@gmail.com

D. Vijaya Bhaskar
devara@iitism.ac.in

R. K. Jisha
jisha.rk123@gmail.com

Ram Krishan
ramkrishan.iitd@gmail.com

R. Gnanadass
gnanadass@pec.edu

1 Department of Electrical Engineering, IIT (ISM) Dhanbad, Dhanbad, India

2 Deloittee Consulting Ltd, Mumbai, India

3 Department of Electrical Engineering, NIT Warangal, Warangal, India

4 Department of Electrical Engineering, Pondicherry Engineering College, Puducherry, India

support [4–6]. Based on its technical merits, usage of Li-ion batteries has been increased in e-mobility [7–10] and grid storage applications [11, 12]. The sizing of Li-ion battery for storage applications and different control strategies for providing PFR has been addressed in [13, 14].

It is expected that the battery can provide enough energy output throughout its life, but its performance reduces considerably due to varying operating temperatures, the number of cycles operated, C-rate and depth of discharge, etc. [15]. Hence, the investigation of performance degradation and lifetime estimation of any battery system is essential when it is used for commercial applications. Recent past, an extensive research has been carried out to study the performance and capacity degradation of Li-ion batteries for various applications [14, 16, 17]. Lifetime estimation, capacity and power fade of $LiFePO_4$ batteries for the electric vehicle applications are presented in [18] and for frequency regulation applications are presented in [19, 20]. These studies have been carried out on an experimental basis by considering synthetic data profiles by assuming the temperature and SOC levels. The performance and the life of the whole battery system depend upon the operational characteristics of an individual cell of the system. The performance of each cell varies concerning to others due to their chemical composition. It is essential to consider the individual cell parameters for accurate lifetime estimation and behavior degradation of a complete battery system when it is deployed in MW scale capacities. Also, the charge/discharge patterns of the grid connected BESS are intermittent in ancillary service applications, especially frequency regulation and RE firming, etc. The behavior of individual cell varies as the frequent variations in charge/discharge patterns. Hence it is also recommended to consider and analyze the individual cell behavior in estimation of capacity degradation and lifetime of large-scale battery systems.

This paper focuses on the performance of individual cell based on operating temperature and SOC variations for different ancillary services. The field data have been considered from the 500 kW/250kWh capacity of the $LiFePO_4$ battery system established by Powergrid at Puducherry in India. The capacity degradation and the life estimation made for individual cells of the system are based on field data inputs and accelerated lifetime models. This paper also investigates the performance of $LiFePO_4$ battery system when it used for FR and ETS applications on various aspects. Recommendations made based on performance analysis and field operating conditions.

The remaining paper is organized as follows. Section 2 provides a detailed methodology of the battery cycle life estimation model. Lifetime estimation for different grid applications and the proposed optimization framework is explained in Sect. 3. Besides, operational challenges of BESS for grid applications are addressed along with recommendations in Sect. 4. The conclusion made is based on the demonstrated system results under Sect. 5.

2 Methodology for life cycle estimation

$LiFePO_4$ batteries are effectively used for various grid applications, especially for ancillary services [21]. The capacity degradation and lifetime of these batteries depend upon its operational conditions and type of applications used [22, 23]. The operating conditions and requirements of each application are unique which requires high level of flexibility and fastness along with the precise control of the sources. It is clear that the battery response time and charge/discharge pattern vary with respect to their utilization [24]. Hence, the estimation of capacity fade and lifetime of any BESS is quite challenging when it comes to grid applications. Also, it is difficult to estimate the battery life on the basis of number of cycles given by the manufactures because of random use of the charging and discharging patterns. Since the charge/discharge patterns are intermittent in ancillary service applications, especially for frequency regulation, counting of number of cycles used per day is not possible precisely. For optimal operation and planning perspective, evaluation of battery health, life cycle and capacity degradation is essential for the BESS operator/ owner for economical operation of the system. The above factors are considered in the proposed methodology and recommendations made for effective deployment of BESS in MW scale across the grid.

The Li-ion battery discharging process is an exothermic reaction while the charging process is an endothermic reaction and in effect, the battery temperature is higher than the initial temperature after completing a charging and discharging cycle. If the temperature of the battery environment is higher, it results in heating of the battery and subsequently the battery temperature increases. During higher temperatures, the battery reactions are aggressive and again increase the battery temperature leading to the thermal runaway, which results in the failure of the cell [25]. The temperature of operation and temperature at which the battery is stored also affect the performance of the battery (Fig. 1).

A novel approach is proposed to estimate the lifetime, capacity degradation and power fade of the $LiFePO_4$ batteries from the SOC, temperature and C- rate which are evaluated using the real-time field operative data. It is assumed that the life of the battery ends when it reached 20% of degradation. Based on the field operating conditions of each application, the life cycles and period of operation in years calculated. $LiFePO_4$ battery technology offers the best balance of energy density and intrinsic safety compared to other Li-ion group of batteries [26]. The parameters which characterize the $LiFePO_4$ batteries are the SOC, Open Circuit Voltage (V_{OC}), C-rate, discharging/charging current, internal

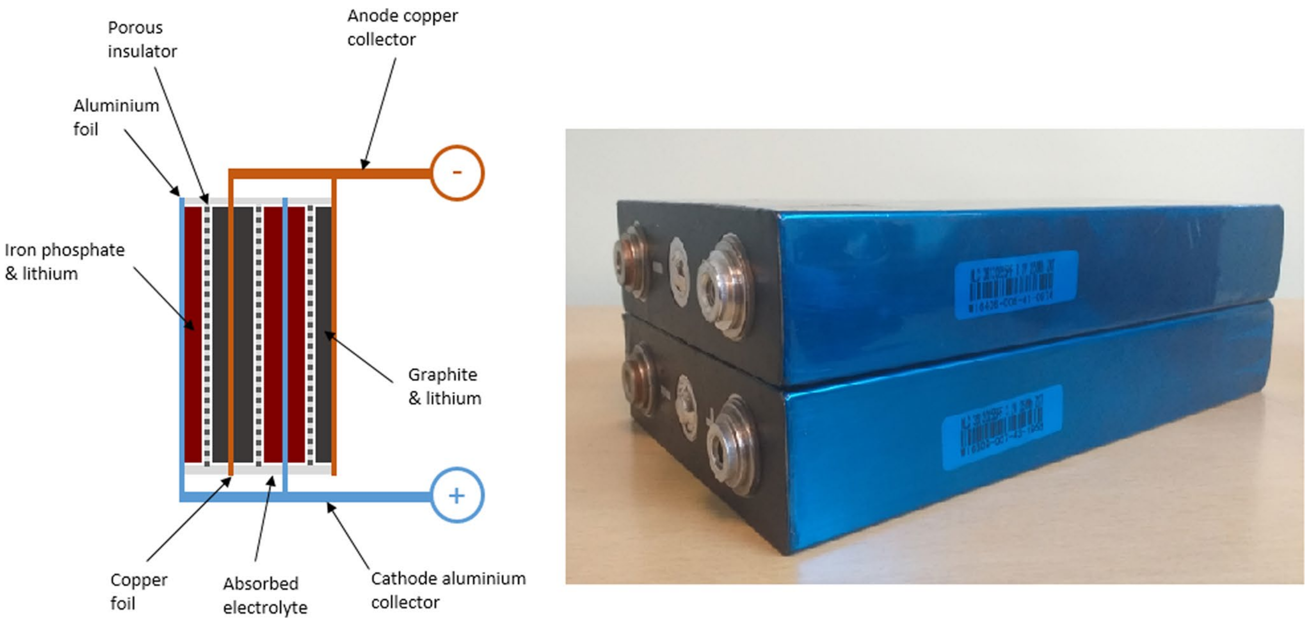

Fig. 1 Lithium iron phosphate battery structure and battery modules

resistance, DOD and temperature (storage and operating) [27–29]. In general the capacity degradation of Lithium-ion batteries can be classified into cyclic aging and calendar aging.

a. Degradation on operation (Cyclic aging)
b. Degradation due to storage (Calendar aging)

2.1 Degradation on operation (cyclic aging)

The cyclic aging of the battery is analyzed by considering the stress factors like operating temperature, the number of cycles, their cycle depths, and the current rate which directly influence the nominal capacity of the battery [30]. Based on design and manufacturing, there is a specific range of temperatures at which the batteries can be used safely, but due to excessive charging and discharging, the probability of variation in temperature is more [31, 32]. This causes more stress in the battery and leads to performance degradation.

Capacity and power fade of the battery due to the cyclic aging ($C_{fade}[\%]$) can be calculated using the empirically derived Eqs. (1) and (2), respectively, which are functions of the number of cycles (*nc*), temperature in Kelvin *(T)* and Cycle Depth (*cd*) of discharge in percentage.

$$C_{\mathrm{fade}}(nc, T, cd) = 0.00024 * \exp^{0.02717 \cdot T} * 0.02982 * cd^{0.4904} * nc^{0.5} \quad (1)$$

The impacts of the of the temperature, cycle depth and the number of cycles on the rate of capacity and power fade of $LiFePO_4$ battery are shown in Fig. 2. For Lithium-ion batteries the most suitable operating temperature is considered as 25 °C and the allowable depth of discharge of the battery while maintaining the health of the battery is 70% as per the manufacturer details of the battery under study. Nominal capacity of the battery is decreasing with increase in the temperature, the changes in the cycle depth and the number of cycles operated. In order to enhance the life of the battery, it has to operate at minimum temperature and optimal SOC/DOD.

2.2 Degradation due to storage (calendar aging)

Li-ion cells do not only degrade as a result of utilization. While on rest, the Solid Electrolyte Interface (SEI) layer exposed to the electrolyte can slowly enhance its growth. The thermodynamic stability of the components and chemical side reactions inside the cell determine the aging rate on storage [33]. Under the right condition, capacity fade can be minimized, but in the case of exposure to elevated temperatures, the activation energy of chemical reactions become lower and aging reactions can occur faster [34].

The capacity degradation due to calendar aging can be calculated from Eq. (3).

$$P_{\mathrm{fade}}(nc, T, cd) = \frac{1}{3}\left(5.78 * 10^{-4} * \exp^{0.03*T} + 1.22 * 10^{-7}\right) * 2.918 * 10^{-5} * \exp^{0.08657*cd} * nc^{(0.00434*T - 0.008*cd - 0.1504)} \quad (2)$$

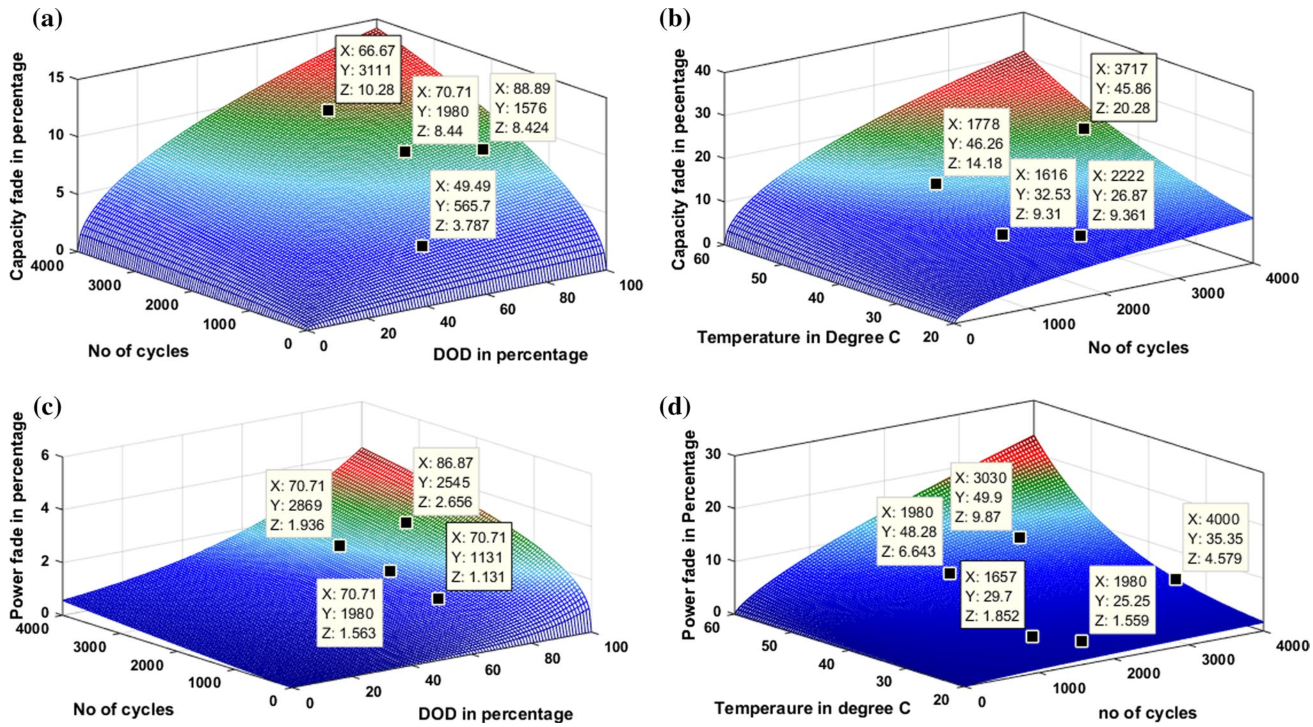

Fig. 2 Cyclic Aging **a**. Capacity fade at 25 °C, **b**. Capacity fade at 70% DOD, **c**. Powers fade at 25 °C, **d**. Power fade at 70% DOD

$$C_{\text{fade}} = \left(0.019 * SOC^{0.823} + 0.5195 * 3.258 * 10^{9} * T^{5.087} + 0.295\right) * \left(t^{0.8}\right) \tag{3}$$

Here the equation is a dependent function of SOC of the battery (in percentage), the duration of storage t (in months) and storage temperature T (°C).

Similarly, the power fade due to the calendar aging mechanism can be defined as

$$P_{\text{fade}} = \frac{0.000375 * SOC + 0.1363}{0.155} * 0.003738 * \exp^{0.06778*T} * t \tag{4}$$

From the results shown in Fig. 3, it is clear that the SOC at which the battery is being stored has a major effect than the storage temperature. The influence of high SOC is more profound during long storage time, but the amount of time spent at certain SOC during cycling can play a role in aging too. If the batteries are stored at 50% SOC, the degradation rate is less when compared to storing at high SOC. In this analysis the capacity degradation of Li ion BESS for both FR and ETS is calculated as a resulted sum of both calendar as well as cyclic aging.

It is verified with real-time SCADA data that, the estimated results through empirical equations are matching with real-time analytics. Hence the applicability of equations holds good for estimation of power fade and capacity degradation for grid scale size battery systems.

3 Capacity degradation in real-time grid applications

The proposed methodology for lifetime estimation of $LiFePO_4$ batteries has been verified with real-time system data. A pilot project has been established by POWERGRID with a capacity of 500 kW/250kWh $LiFePO_4$ battery system connected to EHV grid at Puducherry in India. This system is established to test different applications such as Frequency regulation (FR), Energy time shift (ETS) and RE firming, Reactive power support etc.

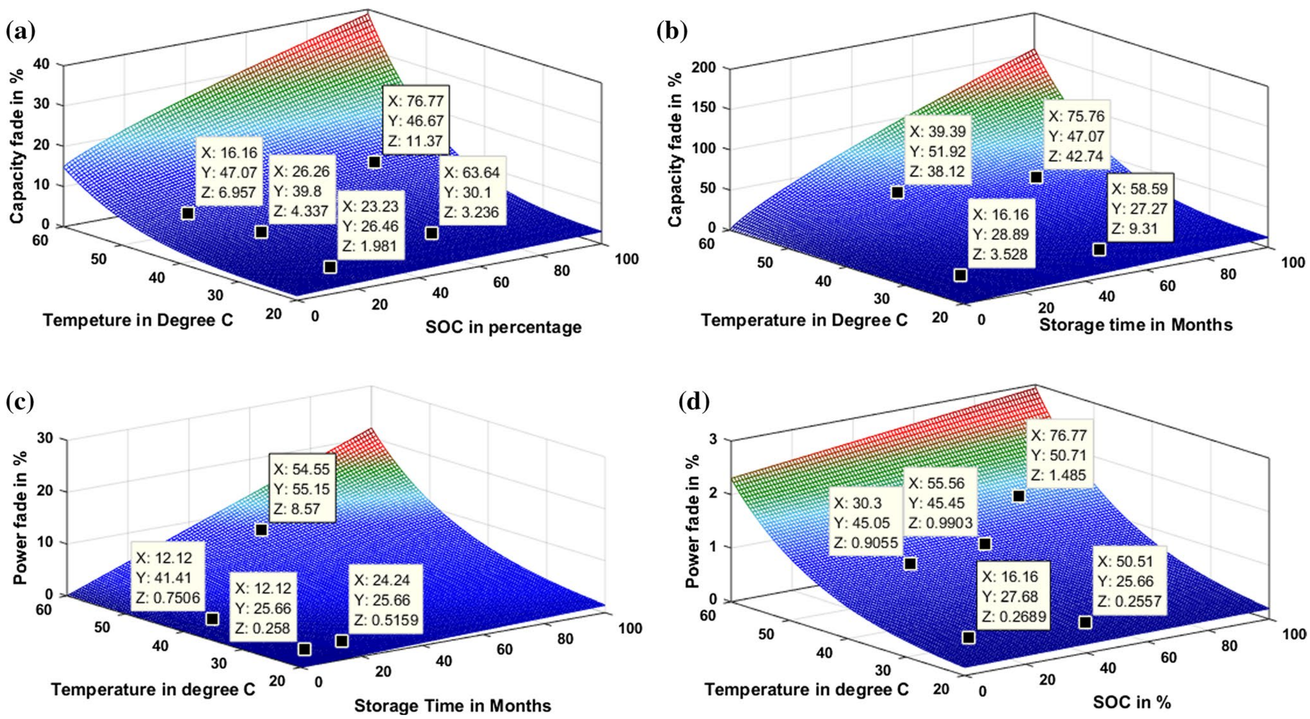

Fig. 3 Calendar Aging—**a** Capacity fade after 1 year of storage, **b** Capacity fade at 50% SOC, **c** Power fade at 50% SOC, **d** Power fade after 1 year of storage

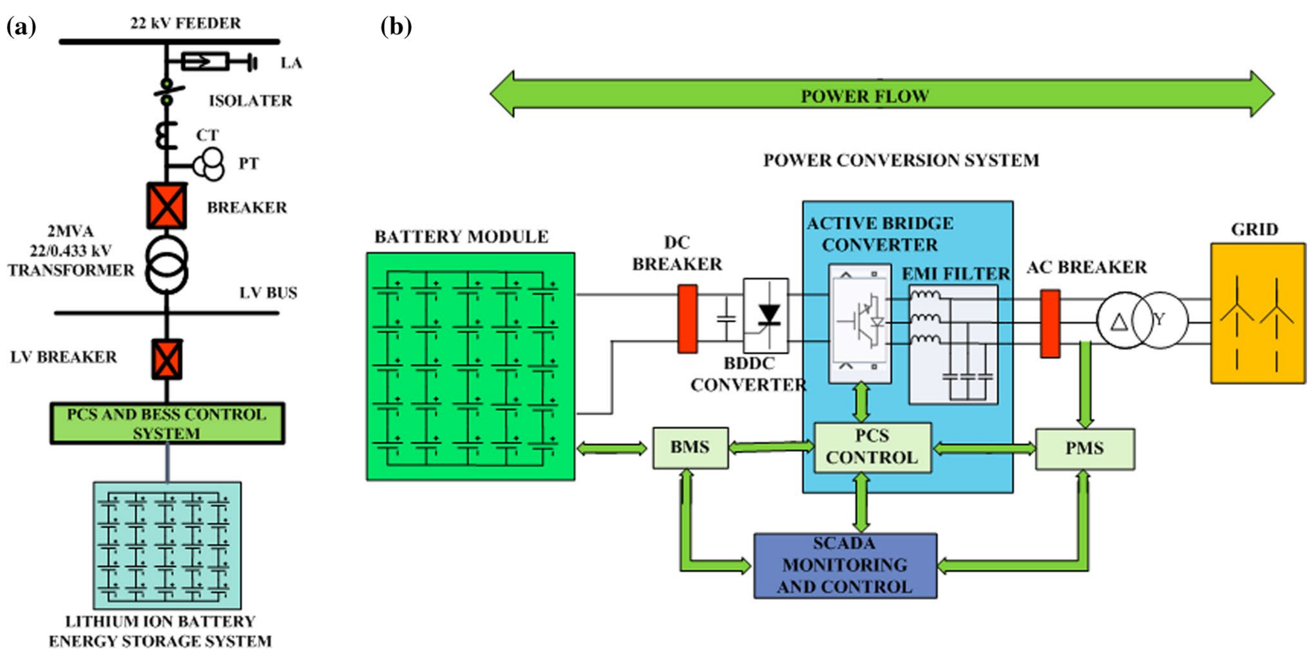

Fig. 4 **a** Single Line Diagram, **b**.Architecture of Battery Energy Storage System

3.1 System architecture

The basic architecture of the Battery Energy Storage System is presented in Fig. 4. It basically consists of Battery modules, Power Conversion System (PCS), Battery Management System (BMS), Power Management System (PMS) and Bay Control Unit (BCU). Technical specifications of $LiFePO_4$ batteries used in this project are mentioned in

Table 1 Technical specifications of the battery under study

Sl. No.	Description	Details
1	Type	Lithium iron phosphate ($LiFePO_4$)
2	Cell voltage	3.2 V
3	Cell capacity	80 Ah
4	Total no. of cells used	1728 Nos
5	Total number of strings/clusters	4 Nos
6	DC Bus/string voltage	691.2 V
7	Total capacity	357 kWh
8	Maximum discharge	500 kW
9	Response time	1 s
10	DOD	70%
11	SOC limits	30–100%

Table 1. Each cell is of 3.2 V and 80Ah capacity. Total 1728 nos. of cells used to get the required capacity. All individual cells are connected in series/parallel combinations and separated into four clusters to get the required capacity. All the clusters are connected to the common DC bus and the DC bus voltage is 691.2 V.

The major components of BESS are:

A. *Power Management System (PMS)* PMS senses the grid frequency and analyze the frequency samples as per control algorithm. Based on the grid frequency, it passes command to PCS for charge/discharge of power to support the grid.
B. *Power Conversion System (PCS)* PCS plays major role in the Battery system. Based on inputs from PMS and BMS, it controls the amount and rate of charge/discharge power. It acts as both AC-DC converters and vice-versa.
C. *Battery Management System (BMS)* BMS plays active role in maintenance of healthiness of battery system. It consists of sensors for measuring individual cell voltage, current, temperature and software for monitoring & control. Total 864 nos. of voltage sensors and 432 nos. of temperature sensors used to monitor real-time parameters of individual cells. It also manages the cell balancing by controlling/restricting charge/discharge power based on operational limits of voltage and temperatures of individual cells. Passive cell balancing methodology is used in this system. BMS broadly classified into Battery monitoring units (BMU), Local/slave BMS units and Master BMS. Battery monitoring units collects all input data such as voltage, temperature, current. from individual cells and communicates to local/slave BMS. Each BMU collects date from group of individual cells. Various numbers of BMUs installed for group of battery clusters. After collection of data from BMUs, the local/slave BMS sends all individual cell data to master BMS. Master BMS analyzes the data and provides commands/signals to PCS for charge/discharge power. BMS will control/restrict the amount of power flow (based on pre-programmed values) in case of any abnormality in individual cell parameters such as voltage and temperatures. BMS also balances the flow of currents among clusters based on the healthiness of the battery packs.

All the control logic performed by the PMS and it provides input signal to PCS for the required amount of charge/discharge power. Bay control unit (BCU) collects all the data from various field devices and communicates to Supervisory Control and Data Acquisition (SCADA) servers for monitoring and control of the entire system. The real-time data have been captured from BMS, PCS and SCADA system for the impact demonstration.

3.2 System analysis

Since the major grid applications of BESS are Frequency Regulation and Energy Time Shift/Peak Shaving, capacity degradation and life cycles estimation of the proposed battery system are estimated for both applications. Field data samples and estimated results presented for both grid applications.

3.2.1 Case 1: frequency regulation

Frequency regulation is one of the significant ancillary services that entail moment-to-moment reconciliation of the difference between supply and demand. During frequency regulation, grid frequency is maintained in the specified band to ensure the stability and reliability of the grid. Coming to the ancillary services, complete commercial guidelines for operating frequency regulation and other services have not yet been established in India, even across the globe. As per grid code regulations, the operational grid frequency in India is 50 Hz and the lower cut off frequency is 49.7 Hz. The allowable operating frequency range is 49.95–50.05 Hz without penalties. In this operation, the frequency control settings for ESS are defined as per grid code regulations as mentioned in Fig. 5. Based on the real-time grid frequency variations, the battery system charges from the grid if the grid frequency is more than 50 Hz and it discharges to the grid if the frequency is less than 49.95 Hz. During SOC mode (between 49.95 and 50 Hz), battery system charges or discharges to maintain optimum SOC (optimum SOC is 80%).

Variation in the Indian grid frequency is more compared to European countries grid frequency variation due

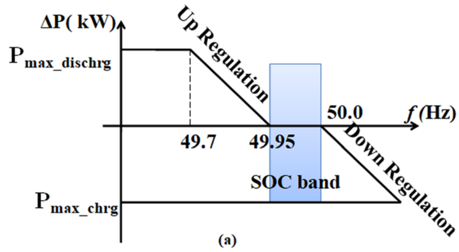

(a)

Sl. No	Frequency range	Operation
1	F< 49.95 Hz	Discharge Mode
2	49.95 < F < 50 Hz	SOC Mode
3	F > 50 Hz	Charging Mode

(b)

Fig. 5 **a** Frequency Regulation Curve, **b** Frequency Regulation Conditions

to various real-time operating conditions. As the variation in the grid frequency is more, the charge/discharge power from BESS also varies continuously as per frequency variation. One-minute interval data of real-time grid frequency, BESS power and SOC for one day have been presented in Fig. 6a. SOC of the battery system measured through BMS software in both frequency regulation and energy time shift application. BMS estimates the SOC based on charge/discharge currents and its operation timings. SOC of each cluster measured separately and integrated with SCADA system for effective monitoring and control. The individual cell voltages and temperatures vary as per the rate of change in power charge/discharge. It also depends on amount and duration of charge/discharge power. Due to continuous variation in grid frequency, the BESS operates either in charge/discharge mode continuously. So, the average temperature of the system is high throughout the day which affects the internal resistance and life of the battery.

The response of the individual cell depends upon its internal chemistry. Each cell has an optimal range of operating voltage and temperature. Some of the weaker cells cannot sustain sudden changes in charge/discharge power. If the cell discharges deeper frequently, its voltage falls below lower limits, and temperature rises accordingly. These cells turn into faulty after a certain period of operation and do not support FR application further. The weaker cells need to make fit either by charging fully or it has to be replaced with healthy/spare cells, if it is faulty permanently. Variations in individual cell temperatures measured during the FR application and are shown in Fig. 6c.

The temperature of each cluster depends on the health of the cells in the said cluster as well as the cooling measure distribution. The overheating of the cells can be caused mainly due to the sudden charge and discharge of the batteries, lack of effective cooling mechanism as well as the presence of poor health cells in the cluster.

The voltage and temperature variation of each battery pack with 15 s interval has been captured through the battery management system. It is clear that the rate at which the batteries undergo capacity fade is different for each individual cell due to temperature variation and chemistry of the cell. Capacity degradation of each individual cell has been estimated for 4000 cycles (as per manufacturer specifications) based on real-time temperature variations under frequency regulation application. Figure 7 presents cluster wise single cell temperature variation and capacity degradation. The effect of charge and discharge operation on each cell is different and hence the variation in capacity degradation as well as the temperature variation. The temperature of each cell during the FR operation is recorded from the BMS of the system and using the data the capacity degradation of individual cell is calculated. The cells having high temperatures tend to degrade fast, as the increase in temperature also accelerate the capacity fade of a cell.

Based on the temperature variation range, the cells have been categorized into three groups and presented in Table 2. Capacity fade and power fade have been calculated for each group of cells. The average capacity degradation under frequency regulation for 4000 cycles of operation is estimated as 14.74%, and power fade is estimated as 4.23%. It is assumed that the life of the battery ends when it reaches 20% of its capacity fade. Based on real-time field data, the total number of life cycles estimated as 5849 cycles and it supports 4 years of calendar years if it is operated under frequency regulation application alone.

3.3 Case 2: energy time shift

Energy time shift (ETS)/Peak shaving is one of the frequently used ancillary services due to increased RE integration. Due to ETS application, the burden on the grid reduced during peak-load hours. Here, the ETS planned based on the load profile of the distribution feeder. Energy gets stored in the battery during off-peak hours and the same discharges during peak hours to share the burden on the grid. Different timings for charge/discharge can be programmed based on load of the distribution feeder. In this study, ten different time slots configured for charge/discharge power based on the load profile of the feeder. It is possible to program the charging, discharging as well as the idle time of the BESS prior to the operation after considering the previous load

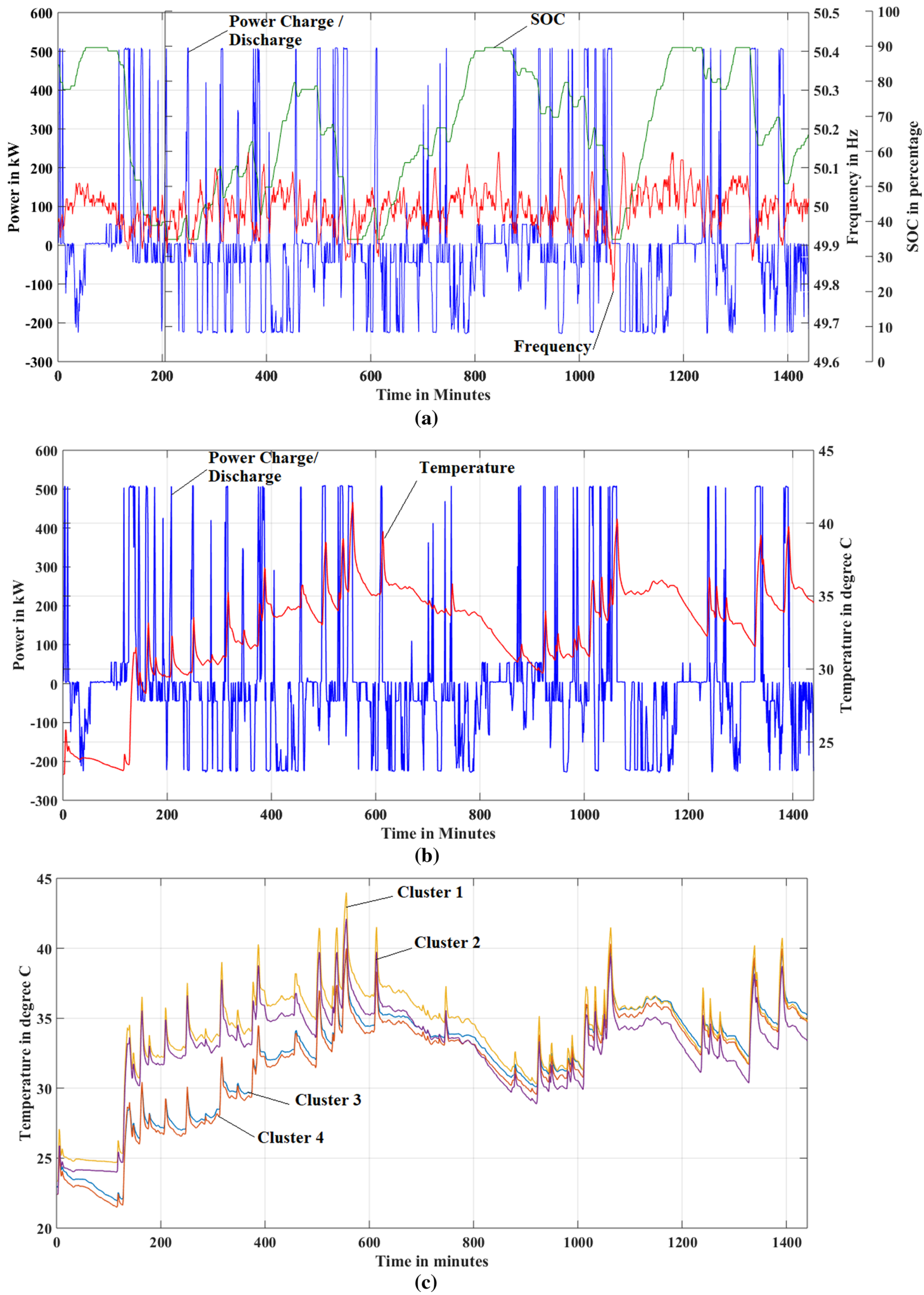

Fig. 6 Frequency Regulation—**a** Power and SOC versus Frequency, **b** Power versus Temperature, **c** Cluster-wise temperatures

CLUSTER 1						CLUSTER 2						CLUSTER 3						CLUSTER 4					
36.21	30.23	37.78	34.06	34.87	29.31	33.69	30.98	38.35	31.88	33.49	30.77	35.62	34.51	39.04	32.62	40.44	32.89	36.42	29.95	37.60	33.65	36.70	32.17
16.19	13.76	16.90	15.27	15.61	13.42	15.12	14.04	17.16	14.39	15.04	13.96	15.93	15.46	17.48	14.68	18.16	14.79	16.28	13.66	16.81	15.10	16.41	14.51
33.13	28.54	34.96	31.50	34.45	29.01	33.56	28.24	37.79	32.58	32.94	28.49	34.96	30.50	36.90	31.80	38.21	29.91	35.24	28.05	35.33	31.18	35.79	29.85
14.89	13.14	15.65	14.24	15.43	13.31	15.06	13.04	16.90	14.67	14.81	13.13	15.65	13.86	16.49	14.36	17.09	13.64	15.77	12.97	15.81	14.12	16.00	13.62
30.22	27.71	30.86	28.63	31.71	28.00	31.11	26.90	35.20	28.85	30.09	27.26	32.45	29.33	33.61	30.24	35.72	28.85	32.69	26.51	32.68	28.51	32.29	28.08
13.76	12.85	14.00	13.18	14.33	12.95	14.09	12.57	15.75	13.25	13.71	12.69	14.62	13.43	15.09	13.76	15.97	13.26	14.71	12.44	14.71	13.13	14.55	12.98
33.71	28.52	37.11	31.81	33.82	28.78	33.49	27.27	35.64	31.55	32.99	27.43	34.84	31.46	37.46	29.72	37.66	31.69	34.65	27.62	36.73	29.87	38.10	28.39
15.12	13.14	16.59	14.36	15.17	13.23	15.04	12.70	15.94	14.26	14.83	12.75	15.60	14.23	16.75	13.57	16.84	14.32	15.52	12.82	16.42	13.63	17.04	13.09
32.35	29.49	34.64	30.45	31.49	29.80	32.54	28.00	35.15	28.95	29.91	29.03	32.62	30.02	37.34	31.37	35.82	31.08	31.63	28.79	37.59	30.45	36.88	29.52
14.58	13.49	15.51	13.84	14.24	13.60	14.65	12.95	15.73	13.29	13.64	13.32	14.68	13.68	16.69	14.19	16.02	14.08	14.29	13.23	16.81	13.84	16.49	13.50
27.98	27.88	28.67	27.79	28.29	29.08	30.20	26.22	29.58	27.23	26.45	27.49	30.05	29.30	32.87	28.40	32.09	28.31	30.00	27.80	33.18	28.03	33.36	31.05
12.95	12.91	13.19	12.88	13.05	13.34	13.75	12.34	13.52	12.68	12.42	12.77	13.69	13.42	14.78	13.09	14.47	13.06	13.67	12.88	14.91	12.96	14.98	14.07
31.64	33.09	36.32	35.20	31.96	34.11	34.60	34.22	36.26	33.38	33.29	37.76	33.26	34.99	37.92	37.95	36.22	36.02	33.87	33.09	37.22	36.32	33.78	34.30
14.30	14.87	16.24	15.75	14.42	15.29	15.50	15.33	16.21	14.99	14.95	16.88	14.94	15.66	16.96	16.97	16.19	16.10	15.19	14.87	16.64	16.24	15.15	15.37
31.96	31.43	33.14	34.99	32.47	32.62	32.29	32.26	33.17	33.21	32.86	33.48	33.15	34.16	35.26	34.86	33.62	34.27	32.59	30.35	34.66	33.50	30.15	32.90
14.42	14.22	14.89	15.66	14.63	14.68	14.55	14.54	14.90	14.92	14.78	15.03	14.90	15.31	15.78	15.61	15.09	15.36	14.67	13.81	15.52	15.04	13.73	14.80
29.35	28.16	28.89	30.36	28.62	30.68	28.33	28.98	28.63	29.40	29.60	30.38	30.63	32.55	31.33	31.50	29.88	29.94	29.95	27.83	31.45	29.21	34.92	30.42
13.44	13.01	13.27	13.81	13.17	13.93	13.07	13.30	13.17	13.45	13.53	13.82	13.91	14.65	14.18	14.24	13.63	13.65	13.66	12.89	14.22	13.38	15.63	13.83
31.49	30.67	33.02	33.92	31.33	29.37	29.68	32.55	33.03	33.37	33.24	29.97	31.97	30.03	34.21	34.14	37.88	32.91	32.25	28.68	35.26	33.08	33.18	31.77
14.24	13.93	14.84	15.21	14.18	13.44	13.56	14.66	14.85	14.99	14.93	13.66	14.43	13.68	15.33	15.30	16.94	14.80	14.54	13.19	15.78	14.87	14.91	14.35
29.76	30.50	31.67	31.35	28.87	31.01	28.64	29.30	31.71	31.41	29.52	30.33	30.32	32.05	32.67	34.49	32.70	32.26	29.62	31.03	32.92	31.91	30.35	31.47
13.59	13.86	14.31	14.19	13.26	14.06	13.18	13.42	14.32	14.21	13.50	13.80	13.80	14.46	14.70	15.45	14.72	14.54	13.53	14.06	14.80	14.40	13.81	14.23
29.23	27.06	27.41	28.28	27.79	28.97	27.98	25.96	27.38	27.80	28.14	27.24	29.24	29.87	30.08	30.83	29.47	29.37	29.38	29.65	31.30	28.82	27.71	28.85
13.39	12.63	12.74	13.05	12.88	13.30	12.95	12.25	12.74	12.88	13.00	12.69	13.39	13.62	13.71	13.98	13.48	13.44	13.45	13.54	14.16	13.24	12.85	13.25
30.06	33.97	33.94	37.02	28.47	35.69	31.00	34.68	32.96	32.92	27.88	33.71	30.37	39.09	33.13	42.05	30.53	39.38	29.28	34.66	31.32	39.79	29.91	38.16
13.70	15.23	15.22	16.55	13.12	15.96	14.05	15.53	14.82	14.80	12.91	15.13	13.81	17.51	14.89	18.97	13.87	17.65	13.41	15.52	14.17	17.84	13.64	17.07
31.49	32.22	31.87	36.53	29.67	33.85	28.46	35.20	30.96	33.78	28.36	31.33	30.68	35.16	32.31	38.90	30.63	39.23	29.92	31.84	31.06	38.99	30.13	35.29
14.24	14.52	14.39	16.33	13.55	15.18	13.12	15.75	14.03	15.15	13.08	14.18	13.93	15.73	14.56	17.42	13.91	17.57	13.64	14.38	14.07	17.46	13.72	15.79
29.32	29.03	29.49	32.08	27.70	31.77	26.24	32.22	30.96	30.68	26.68	29.18	30.68	32.42	30.30	34.17	28.73	34.67	28.26	29.28	28.76	34.29	27.45	32.28
13.42	13.32	13.49	14.47	12.85	14.35	12.35	14.53	14.03	13.93	12.49	13.37	13.93	14.60	13.79	15.32	13.21	15.52	13.04	13.41	13.22	15.37	12.76	14.55
29.86	33.00	30.15	38.77	31.24	33.46	28.17	34.31	30.53	36.28	27.54	35.56	32.03	36.87	31.51	39.01	30.86	37.29	28.80	32.23	30.68	38.91	29.08	36.00
13.62	14.83	13.73	17.35	14.14	15.02	13.01	15.37	13.87	16.22	12.79	15.91	14.45	16.48	14.25	17.47	14.00	16.67	13.24	14.53	13.93	17.42	13.34	16.10
27.77	31.85	29.89	33.66	27.94	34.11	26.33	32.26	30.17	31.40	26.17	32.25	29.21	34.24	29.43	36.67	29.81	35.55	27.54	32.27	29.06	36.08	27.51	34.58
12.87	14.38	13.63	15.10	12.93	15.29	12.38	14.54	13.74	14.21	12.32	14.54	13.38	15.34	13.47	16.39	13.60	15.90	12.79	14.55	13.33	16.13	12.78	15.49
27.81	27.55	28.02	29.13	27.70	31.35	25.61	28.33	28.64	27.79	25.58	28.29	28.06	30.20	28.66	32.67	27.80	32.54	26.75	29.89	26.97	31.08	26.38	32.00
12.88	12.80	12.96	13.36	12.85	14.19	12.14	13.07	13.18	12.88	12.13	13.05	12.97	13.75	13.18	14.70	12.88	14.65	12.52	13.63	12.60	14.08	12.39	14.44

Fig. 7 Heat Map—Average temperature and corresponding capacity degradation of each battery pack for 4000 cycles of operation under FR application (each block—the upper value is average temperature in °C and the lower value is capacity fade in percentage

Table 2 Cluster-wise capacity fade and power fade during frequency regulation for 4000 cycles of operation under FR application (T – operating temperature in °C)

Cluster	T >35 °C		30 °C <T< 35°C		T < 30 °C		Average C_{fade}	Average P_{fade}
	C_{fade}	P_{fade}	C_{fade}	P_{fade}	C_{fade}	P_{fade}		
Cluster 1	16.4218	5.0165	14.5653	3.7484	13.1659	2.9328	14.7177	3.8992
Cluster 2	16.2359	4.8797	14.5702	3.7515	12.9447	2.8146	14.5836	3.8153
Cluster 3	16.802	5.3033	14.5455	3.736	13.3674	3.0431	14.9050	4.0275
Cluster 4	16.5038	5.0776	14.556	7.7426	13.1653	2.9325	14.7417	5.2509
Total degradation under FR application							**14.7370**	**4.2482**

patterns. Once the time slots and amount of energy to be either charged or discharged are decided, the BESS will work accordingly irrespective of the grid conditions. Unlike in FR, in Energy time shift application the battery will have idle states which the capacity fade is mostly due to the calendar aging rather than cyclic aging.

The status of power and SOC are shown in Fig. 8a. Unlike in FR application, BESS supports the grid during peak hours only. The rate of change in power variation and amount of power discharges is also less compared to FR application. Hence, individual cell voltage and temperature variations are minimum. The average temperature w.r.t power and cluster wise temperatures are shown in Fig. 8b, c.

From Fig. 8a, it is clear that the battery either charges or discharges during the allocated timeslots, which is defined in the BESS controller and the remaining time the battery

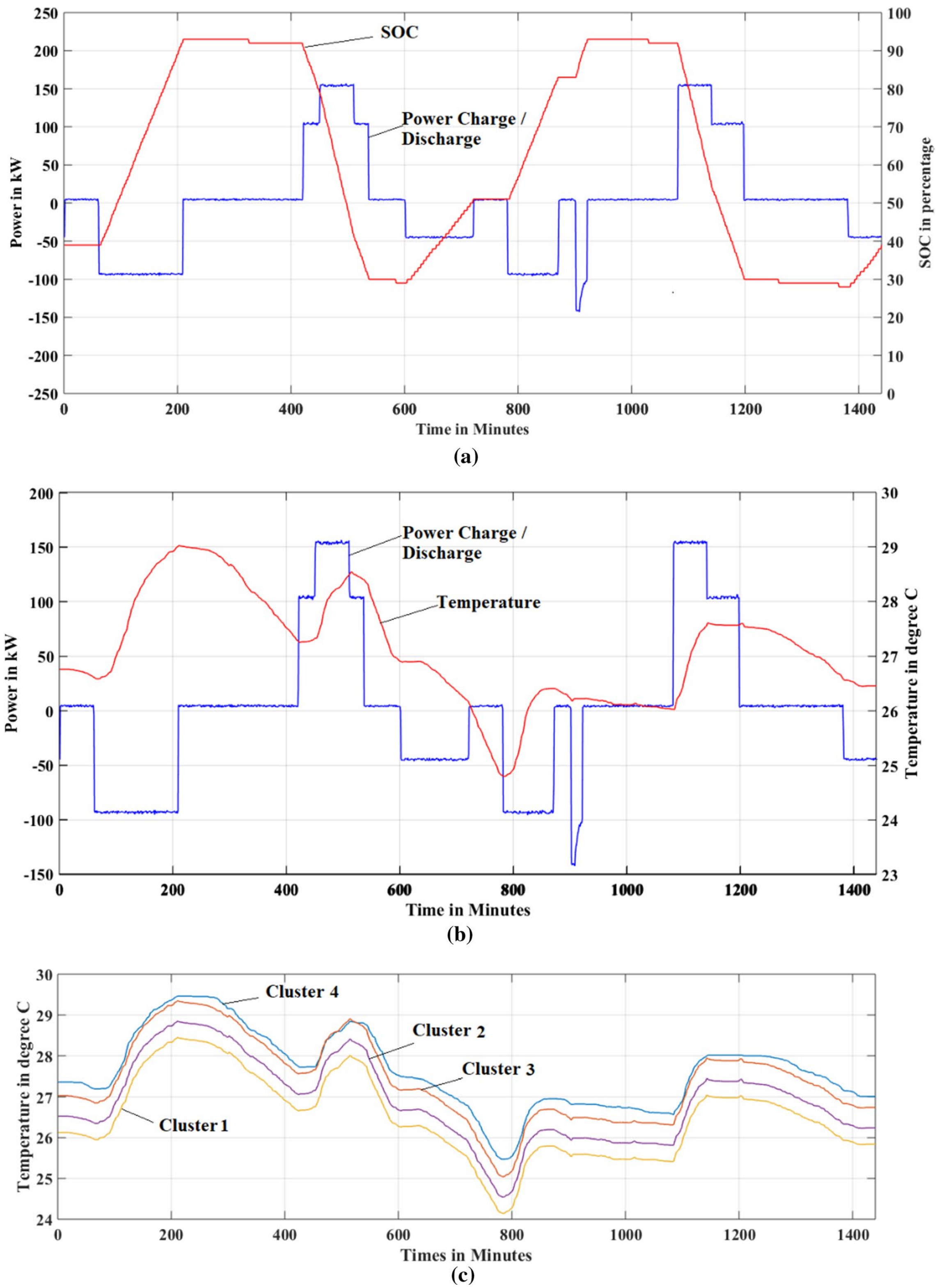

Fig. 8 Energy Time Shift Application – **a** Power versus SOC, **b** Power versus temperature, **c** Cluster-wise temperatures

CLUSTER 1					
21.56	19.28	24.22	21.07	21.94	19.61
13.16	12.44	14.09	13.00	13.29	12.54
21.00	18.78	22.59	20.13	21.80	19.26
12.98	12.29	13.51	12.70	13.24	12.44
19.77	18.60	20.67	18.91	20.95	19.02
12.59	12.24	12.87	12.33	12.96	12.37
20.97	18.97	22.60	20.61	21.27	19.83
12.97	12.35	13.51	12.85	13.06	12.61
20.37	19.57	21.70	20.10	20.43	19.81
12.78	12.53	13.20	12.69	12.80	12.60
19.03	18.95	19.50	19.08	19.31	19.57
12.37	12.34	12.51	12.38	12.45	12.53
20.23	20.76	22.42	21.74	20.48	21.21
12.73	12.90	13.45	13.22	12.81	13.04
20.42	20.12	20.91	21.89	20.72	20.65
12.79	12.70	12.95	13.27	12.89	12.87
19.67	18.84	19.45	19.80	19.37	19.94
12.56	12.31	12.49	12.60	12.47	12.64
20.00	19.68	21.02	21.26	20.18	19.69
12.66	12.56	12.98	13.06	12.72	12.57
19.46	19.69	20.42	20.37	19.01	19.83
12.50	12.57	12.79	12.78	12.36	12.61
19.77	18.60	18.85	19.16	18.86	19.56
12.59	12.24	12.31	12.41	12.32	12.53
19.87	21.25	20.99	24.09	18.95	22.17
12.62	13.06	12.97	14.04	12.35	13.36
19.58	20.66	20.34	23.53	19.68	21.68
12.53	12.87	12.77	13.84	12.56	13.20
18.98	19.74	19.60	21.15	18.79	20.92
12.35	12.58	12.54	13.03	12.30	12.95
19.48	20.49	20.19	24.11	19.97	20.89
12.50	12.81	12.72	14.05	12.65	12.94
18.65	20.27	19.91	21.69	19.01	21.31
12.26	12.75	12.63	13.20	12.36	13.08
18.82	18.93	19.22	19.72	18.94	20.42
12.31	12.34	12.42	12.58	12.34	12.79

CLUSTER 2					
21.42	19.90	25.37	20.19	21.01	19.53
13.11	12.63	14.53	12.72	12.98	12.52
21.24	18.77	24.88	20.54	20.96	18.88
13.05	12.29	14.34	12.83	12.96	12.33
20.33	18.52	22.86	18.99	19.79	18.32
12.76	12.22	13.60	12.36	12.60	12.16
21.09	18.81	22.86	20.48	20.53	18.75
13.01	12.30	13.60	12.81	12.83	12.29
20.59	18.94	22.29	19.51	19.10	19.06
12.85	12.34	13.40	12.51	12.39	12.38
19.73	18.43	20.09	18.84	18.39	18.70
12.58	12.19	12.69	12.31	12.18	12.27
21.25	21.32	22.45	20.91	20.83	21.91
13.06	13.08	13.46	12.95	12.92	13.28
20.76	20.46	21.37	20.82	20.43	20.90
12.90	12.80	13.10	12.92	12.80	12.94
19.35	19.45	19.79	19.58	19.49	19.72
12.46	12.50	12.60	12.53	12.51	12.57
19.65	20.29	21.45	20.40	20.12	19.46
12.55	12.75	13.12	12.79	12.70	12.50
19.14	19.42	20.80	20.01	19.17	19.54
12.40	12.48	12.91	12.67	12.41	12.52
18.96	18.28	19.42	19.01	18.87	18.67
12.35	12.15	12.48	12.36	12.32	12.26
19.46	21.99	20.93	21.07	18.84	20.87
12.50	13.30	12.96	13.00	12.31	12.93
18.91	21.81	20.15	21.41	18.87	20.39
12.33	13.24	12.71	13.11	12.32	12.78
18.18	20.85	20.15	20.20	18.53	19.74
12.12	12.93	12.71	12.73	12.22	12.58
19.14	21.44	20.33	21.85	18.88	21.07
12.40	13.12	12.77	13.25	12.33	13.00
18.42	20.63	19.71	20.06	18.35	20.19
12.19	12.86	12.57	12.68	12.17	12.72
18.32	19.08	19.30	19.17	18.31	19.04
12.16	12.38	12.45	12.41	12.16	12.37

CLUSTER 3					
23.79	22.91	26.60	22.99	25.97	22.84
13.93	13.62	15.03	13.65	14.77	13.59
23.95	21.70	25.29	22.49	25.58	21.88
13.99	13.20	14.50	13.47	14.61	13.26
22.76	20.98	23.17	21.65	23.87	21.10
13.57	12.97	13.71	13.19	13.96	13.01
23.67	21.64	25.10	21.94	24.85	22.27
13.89	13.19	14.42	13.28	14.33	13.40
22.70	21.88	24.81	22.42	24.06	22.51
13.54	13.27	14.31	13.45	14.03	13.48
21.71	21.26	22.62	21.25	22.23	21.24
13.21	13.06	13.52	13.06	13.38	13.05
22.89	23.69	25.10	24.91	23.93	24.00
13.61	13.90	14.42	14.35	13.98	14.01
23.01	23.78	24.08	23.85	23.25	23.40
13.65	13.93	14.04	13.95	13.74	13.79
21.72	22.53	22.23	22.08	21.51	21.46
13.21	13.48	13.38	13.33	13.14	13.13
22.61	21.62	23.52	23.50	23.50	22.76
13.51	13.18	13.83	13.83	13.83	13.56
22.05	22.51	22.76	23.36	22.39	22.86
13.32	13.48	13.56	13.78	13.44	13.60
21.23	21.56	21.51	21.89	21.07	21.39
13.05	13.16	13.14	13.27	13.00	13.10
21.74	25.12	22.76	26.57	21.95	25.40
13.22	14.43	13.56	15.02	13.29	14.54
22.10	23.72	22.60	25.94	21.93	25.13
13.34	13.91	13.51	14.76	13.28	14.44
22.10	22.45	21.48	23.43	20.98	23.07
13.34	13.46	13.13	13.80	12.97	13.68
22.27	23.44	22.60	25.76	22.45	24.25
13.40	13.80	13.51	14.69	13.46	14.10
21.30	23.43	21.83	24.57	21.78	23.74
13.07	13.80	13.25	14.22	13.23	13.91
20.71	21.62	21.10	22.45	20.88	22.25
12.89	13.18	13.01	13.46	12.94	13.39

CLUSTER 4					
23.35	21.60	25.21	22.88	24.81	21.83
13.77	13.17	14.47	13.61	14.31	13.25
23.43	20.96	23.92	21.96	24.46	21.05
13.80	12.96	13.98	13.29	14.18	12.99
22.12	20.15	22.38	20.84	22.58	20.20
13.35	12.71	13.43	12.93	13.50	12.72
23.20	20.65	24.30	21.58	24.76	20.47
13.72	12.86	14.12	13.17	14.29	12.81
22.14	21.29	24.28	21.72	24.15	20.97
13.35	13.07	14.11	13.21	14.06	12.97
21.42	20.80	22.43	20.70	22.70	21.08
13.11	12.91	13.45	12.88	13.55	13.00
22.50	22.74	24.55	24.21	22.82	23.17
13.47	13.56	14.21	14.09	13.58	13.71
22.35	21.84	23.28	23.07	21.20	22.60
13.43	13.25	13.75	13.68	13.04	13.51
21.12	20.73	21.73	21.17	23.59	21.49
13.01	12.89	13.21	13.03	13.86	13.13
22.17	20.84	23.15	22.66	22.64	21.73
13.36	12.93	13.70	13.53	13.52	13.22
21.19	21.80	22.60	22.37	21.46	22.00
13.04	13.24	13.51	13.43	13.13	13.31
20.91	20.95	21.41	21.00	20.40	20.70
12.95	12.96	13.11	12.98	12.79	12.88
21.05	23.29	22.19	28.18	21.28	24.23
12.99	13.75	13.37	15.72	13.07	14.09
21.62	22.26	22.11	27.07	21.36	23.58
13.18	13.39	13.34	15.23	13.10	13.86
20.67	21.09	20.91	23.71	20.33	22.14
12.87	13.01	12.95	13.90	12.76	13.35
21.33	22.16	22.08	25.38	21.19	23.84
13.08	13.36	13.33	14.53	13.04	13.95
20.82	22.39	21.32	23.94	20.45	23.24
12.92	13.44	13.08	13.99	12.80	13.74
20.24	20.92	20.43	21.67	20.07	21.73
12.74	12.95	12.79	13.20	12.68	13.21

Fig. 9 Heat Map—Average temperature and corresponding capacity degradation of each battery pack for 4000 cycles of operation under ETS application (each block—the upper value is temperature and the lower value is capacity fade)

Table 3 Cluster-wise capacity fade and power fade during frequency regulation for 4000 cycles of operation under ETS application (T – operating temperature)

Cluster	Group 1 T > 25°C		Group 2 25 °C < T < 20 °C		Group 3 T < 20°C		Average C_{fade}	Average P_{fade}
	C_{fade}	P_{fade}	C_{fade}	P_{fade}	C_{fade}	P_{fade}		
Cluster 1	0	0	13.0422	1.9885	12.4589	1.7568	12.7448	1.8690
Cluster 2	14.5301	2.6195	12.9847	1.9650	12.3774	1.7253	12.6816	1.8439
Cluster 3	14.6334	2.6652	13.4912	2.1732	0	0	13.6101	2.2231
Cluster 4	14.9718	2.8157	13.3149	2.1000	0	0	13.3703	2.1229
Total degradation							13.1017	2.0147

is in stable state. In order to calculate the capacity degradation of batteries during the ETS application, both cyclic and calendar aging are considered. Since the BESS discharges during peak hours only, the rate of change in variations in individual cell temperature is less.Under this application, capacity degradation of each battery pack has been calculated for 4000 cycles of operation and presented in Fig. 9.

Based on the temperature variation range, the cells have been categorised into three groups and capacity degradation and power fade have been calculated for each group of cells as presented in Table 3. The average capacity degradation under Energy Time Shift application for 4000 cycles of operation estimated as 13.104% and power fade estimated as 2.01%. It is assumed that the life of the battery ends when it reaches 20% of its capacity fade. Based on real-time field data, the total number of life cycles estimated as 6543 cycles and it supports more than 5 years of calendar years if it is operated under energy time shift application alone (Fig. 10).

4 Performance analysis and recommendations

1. At present, BESS are using in various grid scale applications and usage of the battery system is different from each application. It is clear from the above results that, the capacity degradation as well as power fade rate of the battery system during the frequency regulation are much more compared to the energy time shift application. Since the rate of change in charge/discharge power is more and due to continuous operation under FR application, approximately 4 to 5 cycles of energy exchange happen per day. It is estimated that, the total life of the battery operates for 5849 cycles and approximate 4 years of life time under FR operating conditions.
2. In case of energy time shift application, the battery system is allowed for charge and discharge with prior time schedules and also the rate of change in charge/discharge power is less. Since it operates during peak hours, it completes 2 cycles of energy exchange per day. So, it is estimated that, the total life of the battery system is 6543 cycles and operates for more than 5 years under ETS operating conditions. The life of the battery may affect if it is used for combination of different grid applications.

Table 4 Comparison of ETS and FR applications

Sl. No.	Description	FR	ETS
1	Time of operation	Continuous	During peak/ off-peak hours
2	Number of cycles per day	4–5	2
3	Capacity fade	14.7370	13.1017
4	Power fade	4.2482	2.0147
5	Expected life time	4 years	5 years

3. The amount of energy discharge and charge per day of the BESS during ETS is almost the same pattern once the system is programmed with the necessary conditions. In the case of frequency regulation, the amount of energy discharge and charge from the BESS is depends on grid frequency variation and it is very much greater than that of ETS. The comparison of the ETS as well as the FR application is shown in Table 4. The capacity degradation and power fade depend on its operating time and temperatures and amounts of power charge/discharge. As the variations in the grid frequencies are more, the amount of charge/discharge power is more to maintain frequency within the specified limits. Hence, system needs to operate continuously which leads to increase in temperature and finally affects the life of the system.
4. Performance of BESS has been evaluated and the efficiency of the overall system calculated. In general, the major power loss presence in battery modules and minor losses are due to PCS and HT switch gear equipment like Transformer, etc. The overall losses of the system found as 18% excluding auxiliary power consumption. The auxiliary power consumption is for all auxiliary loads such as air condition systems, lighting loads and other local loads of battery container. The auxiliary consumption varies depending upon ambient temperature and type of application also. Due to ambient temperature, the energy consumption for air condition is more during summer period. Since the BESS is under continuous operation during FR application, the temperature of the system is more. Hence the auxiliary power consumption also high to provide proper cooling of the battery system. The average energy consumption of auxiliary system is 4–5%. Hence, the total average loss of the BESS is around 22–24% including auxiliary consumption.
5. As mentioned in above sections, each cell has optimal range of operating voltage and temperatures. The response of the individual cell depends upon its internal chemistry. Some weaker cells may not sustain sudden changes in charge/discharge power. Its voltages and temperatures vary momentarily according to power varia-

Fig. 10 Li-ion battery cells (new cells on left side and used/ faulty cells on right side)

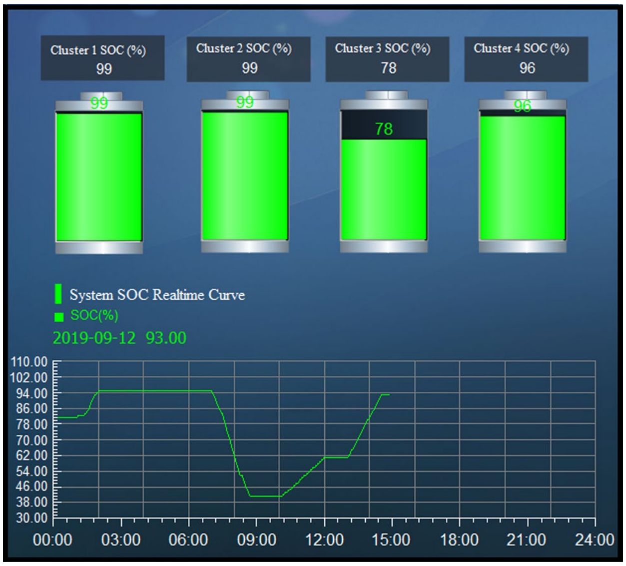

Fig. 11 Uneven SOC of clusters due to continuous operation

tions. These cells become faulty after certain period of operation and it cannot support FR type applications further. Figure 11 shows the new and faulty cells. Due to more temperature variations the cell is bulged and became faulty and it needs to be replaced with healthy/spare cells.

In case of large-scale battery systems (MW scale), thousands of cells used to make the required useful capacity. In such scenario, it is most difficult to attend/replace the faulty cells if it fails frequently. Hence, all the cells in the system need to properly designed and packed to operate efficiently.

6. It has been observed that, after continuous operation, some of the clusters either over charge/discharges which will create unbalance among clusters. BMS plays key role in entire battery storage system. Proper cell balancing taken care by BMS by monitoring individual cell voltage, temperature and SOC. Hence effective BMS system is recommended for efficient operation of BESS. BMS also used to control individual cluster SOCs by monitoring charge/discharge currents.
7. The uneven SOC of clusters (shown in Fig. 11) leads to chances of circulating currents due to variation in cluster voltages which leads to loss of power. Also, the over charged/discharged clusters undergo high currents which create more heat/temperature and leads to degrade earlier compare to other cluster cells.
8. As the temperature of the battery system increases while both charging and discharging modes, air conditioning of the battery container also plays major role. It has been observed that, the temperature of individual cells which are placed at different locations varied differently due to uneven cooling environment. Hence, uniform cooling arrangement has to be provided for all battery cells.
9. If the system operates continuously under ancillary services such as FR application, majority of cells lose its capability to respond sudden change in charge/discharge power after certain period of operation. The variations in voltages are more even if it has higher SOC levels. Hence it is recommended to use the same system for peak shaving or load following type of applications where the rate of change in power variations are less to get maximum utilization of the battery system.

5 Conclusion

Battery Energy Storage Systems are becoming an integral part of the electrical grid to provide ancillary services support as the integration of intermittent renewable energy systems increases into the grid. It is essential to estimate the life cycles and capacity degradation of such BESS which are used in critical grid applications. In this study, the capacity degradation and lifetime of $LiFePO_4$ batteries have estimated when it is used for different grid applications. It is observed that the operational conditions of each application are unique and hence the performance and life of the system also change with respect to the type of application. The lifetime of the system also varies w.r.t usage of the application.

In this study, the capacity fade and lifetime estimation of $LiFePO_4$ batteries have been estimated when it used for FR and ETS applications. The lifetime estimation is formulated based on the accelerated lifetime models considering the real-time operational parameters of the battery such as temperature, State of Charge (SOC), Open Circuit Voltage (V_{oc}) and Depth of Discharge (DOD). A real case installation of 500 kW/250kWh capacity of $LiFePO_4$ battery system into the Indian distribution grid has been considered for the demonstration of the proposed approach. Based on field operational data, it is estimated that the proposed batteries will operate for 5849 cycles and 4 years of timeline under FR application. It will operate for 6543 cycles and more than 5 years of time line under ETS application. The lifetime and capacity vary if it operates for a combination of different grid applications such as FR, ETS, RE firming. The proposed battery life cycle estimation approach shall be used for the design of the size of the battery system for the pre-specified grid applications.

Acknowledgements Authors are thankful to the management of POWERGRID for granting permission for presentation of this paper. Views expressed in the paper are of the authors only and need not necessarily be that of the organization in which they belong.

References

1. Poullikkas A (2013) A comparative overview of large-scale battery systems for electricity storage. Renew Sustain Energy Rev 27:778–788. https://doi.org/10.1016/j.rser.2013.07.017
2. Vazquez S, Lukic SM, Galvan E, Franquelo LG, Carrasco JM (2010) Energy storage systems for transport and grid applications. IEEETrans Ind Electron 57(12):3881–3895. https://doi.org/10.1109/TIE.2010.2076414
3. Hesse HC, Schimpe M, Kucevic D (2017) Lithium-ion battery storage for the grid—a review of stationary battery storage system design tailored for applications in modern power grids. Energies 10:2107. https://doi.org/10.3390/en10122107
4. Stroe D-I, Knap V, Swierczynski M, Stroe A-I, Teodorescu R (2016) Operation of grid-connected lithium-ion battery energy storage system for primary frequency regulation: a battery lifetime perspective. IEEE Trans Ind Appl. https://doi.org/10.1109/TIA.2016.2616319
5. Stroe D-I, Swierczynski M, Stroe A-I (2016) Degradation behaviour of lithium-ion batteries based on field measured frequency regulation mission profile. In: Proceedings of the 2015 IEEE energy conversion congress and exposition (ECCE), Doi: https://doi.org/10.1109/ECCE.2015.7309663
6. Thien T, Schweer D, Stein DV, Moser A, Sauer DU (2017) Real-world operating strategy and sensitivity analysis of frequency containment reserve provision with battery energy storage systems in the german market. J Energy Storage 13:143–163. https://doi.org/10.1016/j.est.2017.06.012
7. Arfeen ZA, Abdullah MP, Hassan R, Othman BM, Siddique A (2020) Energy storage usages: Engineering reactions, economic-technological values for electric vehicles—A technological outlook. Int Trans Electr Energy Syst. https://doi.org/10.1002/2050-7038.12422
8. Hannana MA, Lipu MSH, Hussain A, Mohamed A (2017) A review of lithium-ion battery state of charge estimation and management system in electric vehicle applications: Challenges and recommendations. Renew Sustain Energy Rev 78:834–854. https://doi.org/10.1016/j.rser.2017.05.001
9. Yang J, Dong H, Huang Y, Cai L, Gou F, He Z (2018) Coordinated optimization of vehicle-to-grid control and load frequency control by considering statistical properties of active power imbalance. Int Trans Electr Energy Syst. https://doi.org/10.1002/etep.2750
10. De Gennaroa M, Paffumia E, Martinia G, Giallonardo A (2019) A case study to predict the capacity fade of the battery of electrified vehicles in real-world use conditions. Case Stud Transp Policy. https://doi.org/10.1016/j.cstp.2019.11.005
11. Subburajn AS, Pushpakaran BN, Bayne SB (2015) Overview of grid connected renewable energy based battery projects in USA. Renew Sustain Energy Rev 45:219–234. https://doi.org/10.1016/j.rser.2015.01.052
12. Arteaga J, Zareipour H, Thangadurai V (2017) Overview of lithium-ion grid-scale energy storage systems. Curr Sustain Renew Energy Rep. https://doi.org/10.1007/s40518-017-0086-0
13. Wang D, Ma N, Gao Y, Hu Y, Zhang C (2018) Participation in primary frequency regulation of wind turbines using hybrid control method. Int Trans Electr Energy Syst. https://doi.org/10.1002/etep.2527
14. Das CK, Mahmoud TS, Bass O (2020) Optimal sizing of a utility-scale energy storage system in transmission networks to improve frequency response. J Energy storage 29:101315. https://doi.org/10.1016/j.est.2020.101315
15. Stroe A-I, Knap V, Stroe D-I (2018) Comparison of lithium-ion battery performance at beginning-of-life and end of-life. Microelectron Reliab. https://doi.org/10.1016/j.microrel.2018.07.077
16. Datta U, Kalam A, Shi J (2019) The relevance of large-scale battery energy storage (BES) application in providing primary frequency control with increased wind energy penetration. J Energy Storage 23:9–18. https://doi.org/10.1016/j.est.2019.02.013
17. Nejada S, Gladwina DT, Stone DA (2016) Systematic review of lumped-parameter equivalent circuit models for real-time estimation of lithium-ion battery states. J Power Sources 316:183–196. https://doi.org/10.1016/j.jpowsour.2016.03.042
18. Swierczynski M, Stroe D-I, Stan A-I, Teodorescu R, Kær SK (2015) Lifetime estimation of the nanophosphate LiFePO4/C battery chemistry used in fully electric vehicle. IEEE Trans Ind Appl. https://doi.org/10.1109/TIA.2015.2405500
19. Xu B, Oudalov A, Poland J, Ulbig A, Andersson G (2014) BESS control strategies for participating in grid frequency regulation. In: 19th world congress of the international federation of automatic control, Cape Town, South Africa, https://doi.org/10.3182/20140824-6-ZA-1003.02148
20. Shen J, Dusmez S (2014) Optimization of sizing and battery cycle life in battery/ultracapacitor hybrid energy storage systems for electric vehicle applications. IEEE Trans Ind Inf. https://doi.org/10.1109/TII.2014.2334233
21. Lawder MT, Suthar B (2014) Battery energy storage system (BESS) and battery management system (BMS) for grid-scale applications. Proc IEEE. https://doi.org/10.1109/JPROC.2014.2317451
22. Liu D, Xie W, Liao H (2015) An integrated probabilistic approach to lithium-ion battery remaining useful life estimation. IEEE Trans Instrum Meas. https://doi.org/10.1109/TIM.2014.2348613
23. Fatha JP, Dragicevica D, Bittela L (2019) Quantification of aging mechanisms and in homogeneity in cycled Lithium-ion cells by differential voltage analysis. J Energy Storage 25:100813. https://doi.org/10.1016/j.est.2019.100813I
24. Jha S, Sen S, Tiwari M, Singh MK (2014) Control strategy for frequency regulation using battery energy storage with optimal utilization. In: IEEE 6th India international conference on power electronics https://doi.org/10.1109/IICPE.2014.7115796.
25. Wang Q, Zhao X, Ye J, Qiujuan Su, Ping P, Sun J (2016) Thermal response of lithium-ion battery during charging and discharging under adiabatic conditions. J Therm Anal Calorim 124:417–428. https://doi.org/10.1007/s10973-015-5100-4
26. GhassanZubi R-L (2018) Monica Carvalhob, GuzayPasaoglue, The lithium-ion battery: State of the art and future perspectives. Renew Sustain Energy Rev 89:292–308. https://doi.org/10.1016/j.rser.2018.03.002
27. Xu B, Andersson G (2016) Modeling of lithium-ion battery degradation for cell life assessment. IEEE Trans Smart Grid. https://doi.org/10.1109/TSG.2016.2578950
28. Guo S, Xiong R, Shen W, Sun F (2019) Aging investigation of an echelon internal heating method on a three electrode Lithium-ion cell at low temperatures. J Energy Storage. https://doi.org/10.1016/j.est.2019.100878
29. Meng J et al (2018) An overview and comparison of online implementable SOC estimation methods for lithium-ion battery. IEEE Trans Ind Appl 54(2):1583–1591. https://doi.org/10.1109/OPTIM.2017.7975030
30. Uno M, Kukita A (2015) Cycle life evaluation based on accelerated aging testing for lithium-ion capacitors as alternative to rechargeable batteries. IEEE Trans Industr Electron. https://doi.org/10.1109/TIE.2015.2504578
31. Tripathy Y, McGordon A, Low CTJ (2018) A new consideration for validating battery performance at low ambient temperatures. Energies 11:2439. https://doi.org/10.3390/en11092439
32. Rivera-Barrera JP, Muñoz-Galeano N, Sarmiento-Maldonado HO (2017) SoC estimation for lithium-ion batteries: review and future

challenges. Electronics 6:102. https://doi.org/10.3390/electronics6040102
33. Stroe DI, Swierczynski M, Kær SK, Teodorescu R (2017) A comprehensive study on the degradation of lithium-ion batteries during calendar ageing: the internal resistance increase. IEEE Trans Ind Appl. https://doi.org/10.1109/ECCE.2016.7854664
34. Sarasketa-Zabala E, Gandiga I, Rodriguez-Martinez L, Villareal I (2014) Calendar ageing analysis of a LiFePO4/graphite cell with dynamic model validations: Towards realistic lifetime predictions. J Power Sources 272:45–57. https://doi.org/10.1016/j.jpowsour.2014.08.051